Spin-phonon interaction in small particles of MgO:Ni^{2+}

R. Gallay and J. J. van der Klink
Institut de Physique Expérimentale, Ecole Polytechnique Fédérale de Lausanne, CH-1015 Lausanne, Switzerland
(Received 19 October 1987)

In a crystal of finite size, the frequency of the lowest normal-mode vibration is not arbitrarily close to zero. Well-known theoretical consequences of this gap in the phonon spectrum are an Einstein-like specific heat at extremely low temperatures and a vanishing direct-process electron-spin-lattice relaxation for paramagnetic impurities in small crystals. For the case of MgO we survey calorimetric data from the literature, and present detailed ESR experiments on Ni^{2+} impurities in loose aggregates of small particles, in search of experimental evidence for these effects. For unknown reasons, the result is negative.

I. INTRODUCTION

The first discussions of what is now called a "quantum size effect"[1] were given in 1921 by Schaefer[2] and by Planck,[3] concerning the temperature variation of the specific heat at extremely low temperatures. Schaefer has introduced the concept of a "single-mode regime" for particles containing N' atoms of a substance with Debye temperature Θ_D. He argued that below a temperature $\Theta_0'=\Theta_D(3N')^{-1/3}$ the specific heat should no longer follow Debye's T^3 law, but drop exponentially with the temperature, as in Einstein's treatment of the specific heat. He calculated that for carbon clusters containing $N'=2\times10^3$ atoms in the diamond structure, the single-mode regime should dominate below $\Theta_0'=100$ K.

Experimental data available so far[4–10] never show this single-mode regime: in fact, the low-temperature specific heat of small particles is generally found to be enhanced with respect to that of the bulk; as an example we show data for MgO taken from the literature in Fig. 1. Such an enhancement has been calculated by lattice-dynamical methods for rectangular clusters containing $6\times6\times5=180$ and $10\times10\times9=900$ ions (nearly cubes of sides 10 and 19 Å);[11] no evidence for the single-mode regime, expected below 116 and 67 K, respectively [using $\Theta=945$ K for MgO (Ref. 7)], was found in these calculations (where, however, it may have been masked by effects due to rotational degrees of freedom). Using a continuum model, an enhancement of the specific-heat quadratic in the temperature may be predicted in an intermediate regime where the improved asymptotic Debye's formula is valid.[12,13] At lower temperature and for very small particles, a rigorous Bose-Einstein summation of the vibrational modes shows the drop first mentioned by Schaefer. We have calculated the specific heat of a MgO cube of sides of 400 Å by Bose-Einstein summation of the $3N$ vibrational modes with clamped boundary conditions. The result is presented in Fig. 1.

An effect related to the single-mode behavior of the specific heat, but not requiring extremely low temperatures, has been discussed by Stoneham:[14] he considered the "direct-process" electron-spin-lattice relaxation of a paramagnetic impurity placed in a small dielectric particle. (We will present an elementary derivation of the relaxation time in the next section.) However, at that time the agreement between theoretical predictions and experimental results for direct-process spin-lattice relaxation very often was rather poor,[15] which apparently has discouraged experimental verification of this proposal:

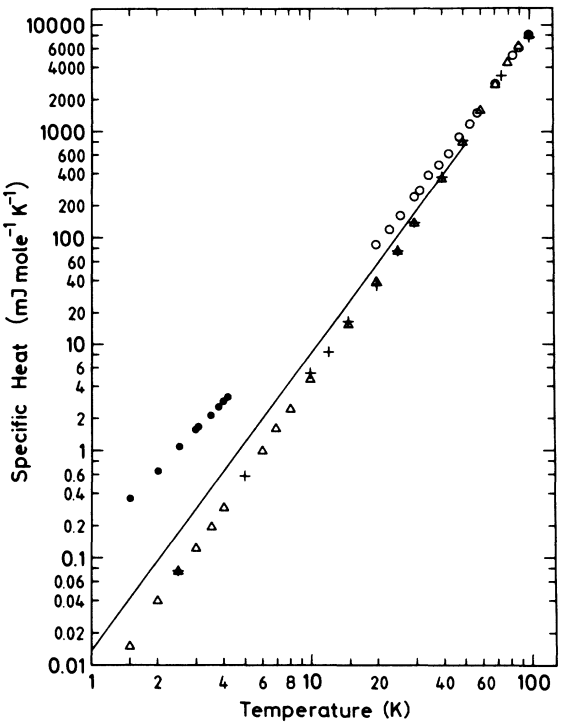

FIG. 1. Specific heat of bulk and small particles of MgO between 1 and 100 K. The small particles have an enhanced (as predicted for the quantum size regime) rather than a diminished (as expected in the single-mode regime) specific heat with respect to the bulk. Since in Debye theory the specific heat of a d-dimensional system varies as T^d, the enhancement should be a surface effect. Data deduced from Ref. 5 (○), Ref. 6 (●), Ref. 7 (+), and Ref. 8 (△). The solid line corresponds to the present theoretical determination for cubes of sides of 400 Å.

the present paper reports, to the best of our knowledge, the first such attempt (albeit with a negative result).

II. THEORETICAL

For comparison between theoretical and experimental values of spin-lattice relaxation time T_1, the dynamic spin Hamiltonian formalism is the most suitable.[16] It is based on a long-wavelength approximation for the phonons; the parameters appearing in the Hamiltonian can then be measured statically and no further theoretical approximations are necessary. (Therefore disagreement between experiment and theory is almost surely due to experimental problems.)

It may be instructive, however, to present a simple derivation based on semiclassical (all variables except spin treated classically) arguments. In fact, the energy of the phonons considered (9 GHz) is much smaller then the thermal energies in our experiment (4.2 K and above); the effect we look for is a "size effect" because of boundary conditions (particles smaller than ~ 3200 Å cannot sustain a 9-GHz phonon) but not so much a "quantum effect" (in the sense that deviations from Boltzmann's statistics play an important role).

In the classical harmonic solid, the motion of each ion is a superposition of normal modes. During vibration, the ions leave their nominal perfectly cubic sites, thus dynamically altering the crystal-field energy of the electron that bears the spin under consideration. Through spin-orbit interaction, the spin itself is affected by the vibration. Therefore we find a time-dependent part in the spin Hamiltonian, capable of inducing transitions between the different energy levels of the static part of the spin Hamiltonian.

The effect on the crystal field in the origin of the ith neighbor ion at instantaneous distance $R_{oi}(t)$ is proportional to some negative power n of the distance. We approximate

$$R_{oi}^{-n}(t)=r_{oi}^{-n}[1-nu_{oi}(t)/r_{oi}] \tag{1}$$

where

$$\mathbf{R}_{oi}(t)=\mathbf{r}_{oi}+\mathbf{u}_{oi}(t)=(\mathbf{r}_o-\mathbf{r}_i)+[\mathbf{u}_o(t)-\mathbf{u}_i(t)] \tag{2}$$

and the index o applies to the ion carrying the spin; in the following we will take it to be in the origin. In the harmonic approximation, $u_{oi}(t)$ is given by

$$\mathbf{u}_{oi}(t)=\sum_k \mathbf{e}_k \exp(i\omega_k t)^*[1-\exp(i\mathbf{r}_i\cdot\mathbf{k})] . \tag{3}$$

Anticipating that we will use only low-frequency modes, we make a long-wavelength approximation:

$$\mathbf{u}_{oi}(t)/r_{oi}=-i\sum_k \mathbf{e}_k \,|\,\mathbf{k}\,|\exp(i\omega_k t) \tag{4}$$

where for simplicity we have set $\mathbf{k}\cdot\mathbf{r}=kr$.

In the Bloembergen, Purcell, and Pound (BPP) type of time-dependent perturbation theory, the fluctuating interaction in Eq. (1) will give a spin-lattice relaxation rate T_1^{-1} that is proportional to the power spectral density $J_u(\omega)$ of the fluctuation in Eq. (4) at the Larmor frequency ω in thermal equilibrium.

Consider a single harmonic oscillator:

$$x(t)=\exp(i\omega_k t) . \tag{5}$$

The corresponding power spectral density $J_x(\omega)$ is

$$J_x(\omega)=\int_{-\infty}^{+\infty}\langle x(t)x^*(t+\tau)\rangle\exp(i\omega\tau)d\tau \tag{6}$$

where the angular brackets denote a thermal average. Then

$$\begin{aligned}J_x(\omega)&=\int_{-\infty}^{+\infty}\langle x^2(t)\rangle\exp[i(\omega-\omega_k)\tau]d\tau\\&=\frac{k_BT}{m\omega_k^2}\delta(\omega-\omega_k) .\end{aligned} \tag{7}$$

The motion described in Eq. (4) is a superposition of independent oscillatory motions like Eq. (5). Therefore its spectral density $J_u(\omega)$ is a superposition of spectral densities like Eq. (7):

$$J_u(\omega)=\sum_k d_k k^2\frac{k_BT}{m\omega_k^2}\delta(\omega-\omega_k) \tag{8}$$

where d_k is the degeneracy (number of modes with the same $|\,\mathbf{k}\,|$).

The long-wavelength dispersion relation is

$$\omega_k=c\,|\,\mathbf{k}\,| \tag{9}$$

so that we obtain

$$T_1^{-1}\propto J(\omega)=\frac{k_BT}{mc^2}g(\omega) \tag{10}$$

where we introduced the mode density

$$g(\omega)=\sum_k d_k\delta(\omega-\omega_k) . \tag{11}$$

Due to anharmonic effects and to the presence of the surface, the modes will actually not be infinitely sharp (δ functions) but broadened (e.g., Lorentzians).[17]

This semiclassical derivation is valid for $h\omega/kT<1$ and $g(\omega)>0$: it corresponds in a quantum-mechanical derivation to the case where induced emission and absorption are much more important than spontaneous emission.

From the dynamic spin Hamiltonian for Ni^{2+} in MgO it is found that relaxation occurs in general with two time constants.[18] By suitable preparation of the spin system (see Sec. III) only the longer one is observed, the value of which is predicted to be

$$T_1=0.19\tanh\left[\frac{0.22}{T}\right] s \tag{12}$$

in a single crystal, with little (about 6%) variation with orientation.[18] The high-temperature limit of Eq. (12) is

$$T_1T=4.3\times10^{-2}\ \text{s K} \tag{13}$$

[similar in structure to Eq. (10)] and the low-temperature ($T\ll0.22$ K) limit is

$$T_1=0.19\ \text{s} . \tag{14}$$

For MgO:Ni^{2+} the latter temperature region has not experimentally been studied, but it describes the regime where the thermal population of 9-GHz phonons goes to zero, so that spin relaxation proceeds mainly through spontaneous emission of phonons.

In a certain sense, spin relaxation is a two-step process; in the first step energy is transferred from the spins to the phonons of the corresponding frequency; in the second step from the phonons to the thermostat bath. Limitations in their heat capacity and the rate they can transfer energy to the thermostat can increase the temperature of the "corresponding" phonons to above that of the thermostat bath. In the overall transfer of energy from spins to thermostat, this "phonon bottleneck" can become the limiting factor. Selective heating of the corresponding phonons by heavy saturation of the spin system in MgO:Ni has been demonstrated experimentally by Brya, Geschwind, and Devlin.[17]

Under conditions of our experiment, we expect the Faughnan-Strandberg equations[19] to hold. These say that for a saturation-recovery experiment and T_1 much longer than the phonon lifetime the initial decay time constant will be T_1, and the final time constant $T_1(1+\sigma)$ where σ is the bottleneck factor that describes the effect of "selective heating." How long the "initial" portion lasts is determined by σ and by the ratio of T_1 and the phonon lifetime. For an accurate determination of T_1 one needs a sufficiently long initial portion of the decay, or, even better of course, $\sigma \ll 1$. In terms of spins/G, the concentration in our samples is 2 orders of magnitude below that used by Brya *et al.*;[17] in addition, for powders the phonon lifetime should be shorter, further diminishing the bottleneck problem. Therefore we expect to be able to determine T_1 correctly from the experimental decay curves.

In small particles, the cutoff in the phonon spectrum will make the 9-GHz radiation density in the phonon bath equal to zero at all temperatures; therefore relaxation by induced absorption and emission will certainly be inhibited. There might still be spontaneous emission of a quantum of lattice vibrational energy $\hbar\omega_0$, but since there is no corresponding stationary state of the lattice, this quantum has either to be reabsorbed by the spin system or to be transmitted immediately to the thermostat bath. If only reabsorption occurs, the electron spin-lattice relaxation time T_1 will be infinite; if there is only transmission to the bath, the value of T_1 will be given by Eq. (14). In either case, the relaxation will be very slow compared to values predicted by Eq. (13), at least for temperatures above 4 K. Therefore we expect to see in small particles relaxation by two-phonon processes, with their characteristic temperature dependence, down to very low temperatures.

III. EXPERIMENT

A. Single crystal

The cw ESR spectrum of Ni^{2+} in MgO is well known.[20] We will restrict our attention to the "normal" single-quantum, $\Delta M = 1$, transition. Its linewidth in a good crystal doped with 0.01 at. % Ni^{2+} is of the order of 60 G, nearly independent of crystal orientation, and is ascribed to inhomogeneous broadening by dislocations.[21] The homogeneous linewidth is estimated from T_2 measurements to be approximately 20 mG, so that it is not too difficult to obtain a microwave magnetic field component larger than this width, as required for meaningful relaxation experiments. As we have shown earlier[22] (note, however, an error in the caption of Fig. 5 in this reference; the drawn line A is an experimental,[23] not a theoretical result) perfect agreement between theoretical [Eq. (12)] and experimental (Fig. 2) values is obtained by using pulse sequences that ensure sufficient saturation. That the experimental anisotropy of the spin-lattice relaxation is small follows from comparison of the data on the crystal and on a powder ground from it (see Fig. 2).

The values we find for the spin-lattice relaxation time T_1 between 4.2 and 7 K are an order of magnitude larger than those found by Jones and Lewis,[23] but both experiments give the characteristic $T_1^{-1} \propto T$ temperature dependence. We suggest that the difference is due to insufficient saturation (cf. the experimental section), so that the relaxation rates measured earlier were sums of a temperature-independent cross relaxation (or spectral diffusion) and a direct-process relaxation. In that case the temperature variation of T_1 would be correct, but the values too small.

The crystal we used has been grown at Oak Ridge Na-

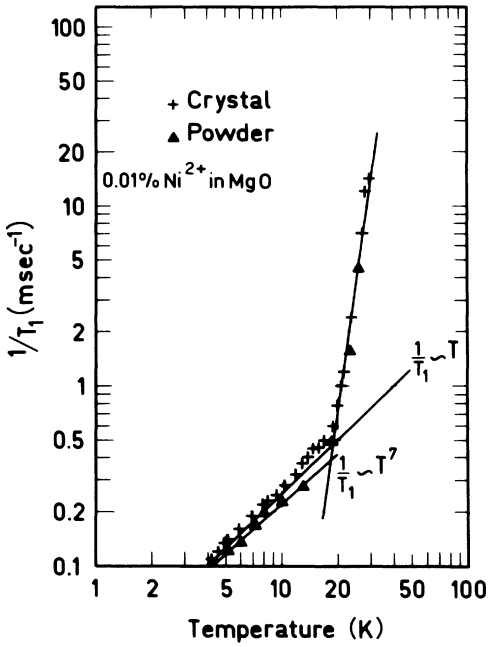

FIG. 2. Electron-spin-lattice relaxation rate T_1^{-1} for Ni^{2+} in bulk MgO. Concentration 10^{-4}. +: single crystal, field along [100]. ▲: powdered crystal. Below 20 K, the slope of 1 is characteristic for the single-phonon direct process and the drawn line represents the theoretically expected values for the single crystal; the slope of 7 indicates the two-phonon Raman process.

tional Laboratory; its nominal Ni content was 10^{-4}; the ESR spectrum indicated additional Cr^{3+} and Mn^{2+}, but little Fe^{2+}.

B. Fine powders

Nickel-doped MgO ultrafine particles have been prepared by two different methods. The first one is a chemical process starting from the magnesium (33 g) and nickel (0.004 g) chloride salts dissolved in 1 l of pure water. The nickel chloride concentration is determined to find a proportion of one nickel for 10^4 magnesium atoms. A solution of 10^{-2} M potassium hydroxide is slowly added to get the greatest number of nucleation germs during the formation of $Mg(OH)_2$:Ni^{2+} and KCl. The hydroxide slowly precipitates while the KCl remains in solution. After filtering and repeated washing, thermal decomposition of the precipitate at 400 °C is achieved.[24] The mean particle size increases by subsequent annealing at higher temperature or for a longer time.

The second method is a laser beam gas evaporation which is a combination of the gas-evaporation technique described by Rappaz *et al.*[25] and the laser-evaporation method by Kato.[26] The compressed MgO:Ni^{2+} powder, initially produced by thermal decomposition, is locally evaporated by a 30-W focused infrared laser beam. A fast thermalization of the vapor atoms occurs in the transporting flow of pure argon gas which is aspirated through a liquid-nitrogen trap by a 12-m^3/h rotary pump. The small particles are collected on a quartz target placed in the middle of the collimated flow. The working conditions are an argon flow rate of 100 sccm (cubic centimeters per minute at standard temperature and pressure) and pressure in the evaporation chamber of 10 torr. Evaporation time for a typical ESR sample was of the order of 1 h.

Electron micrographs of three samples studied are shown in Fig. 3. The tendency of the particles to cluster together has been observed in many other dielectric, semiconductor, or metallic small-particle systems.[25] The shapes of the particles are generally cubelike (as has been observed before), but perhaps less so for the laser-evaporated sample. Since it might well be that the equilibrium shape is more or less spherical we cannot say which method yields particles closet to equilibrium.

The thermal decomposition reaction requires atomic rearrangements, and therefore is expected to create a considerable amount of crystal defects. Indeed we find that the ESR linewidth in these powders may be decreased considerably by annealing. Unfortunately, some increase in size is provoked as well (Fig. 4). In comparison, the lines in the laser-evaporated samples were narrower (than in the decomposed samples) for the same average particle size, showing better crystallite quality.

C. ESR data

The cw ESR spectra for three small-particle samples of average size 170, 270, and 1000 Å are given in Fig. 5. As remarked before, the laser-evaporated sample shows a comparatively narrow line. Indicated on the spectra are the positions in the line where the spin-lattice relaxation

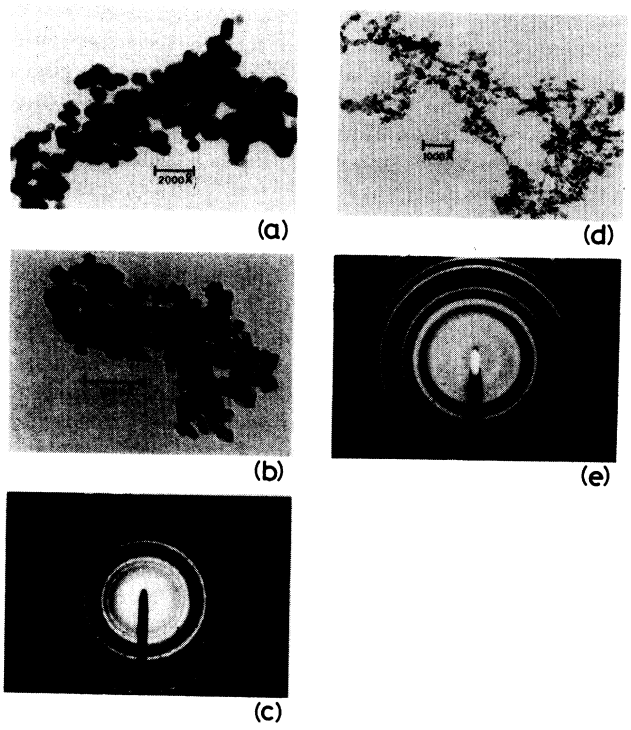

FIG. 3. Electron micrographs and diffraction rings for small-particle samples of MgO:Ni^{2+} prepared by thermal decomposition and by laser evaporation. (a) Thermal decomposition and annealing at 600 °C, average particle size 1000 Å. (b) Thermal decomposition and annealing at 400 °C, average particle size 270 Å. (c) Diffraction rings of the sample shown in (a). (d) Laser evaporation, average particle size 170 Å. (e) Diffraction rings of the sample shown in (d).

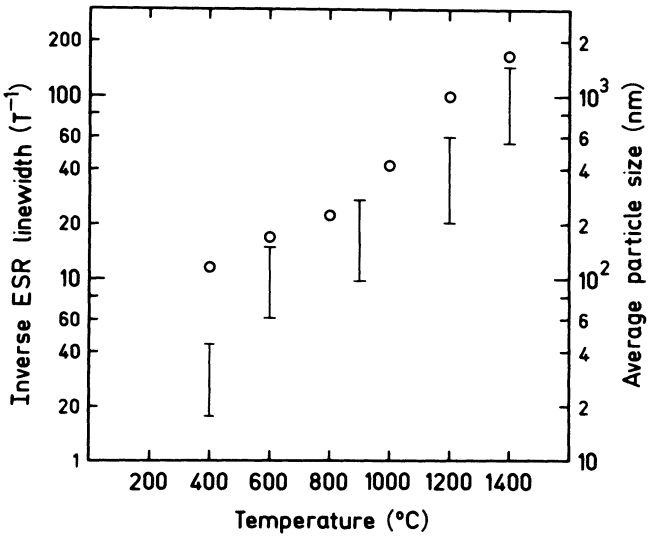

FIG. 4. Inverse ESR linewidth (○) and average particle size (I) of small MgO:Ni^{2+} particles, prepared by thermal decomposition, as a function of annealing temperature. Concentration 10^{-3}. The annealing time is 2 h in all cases.

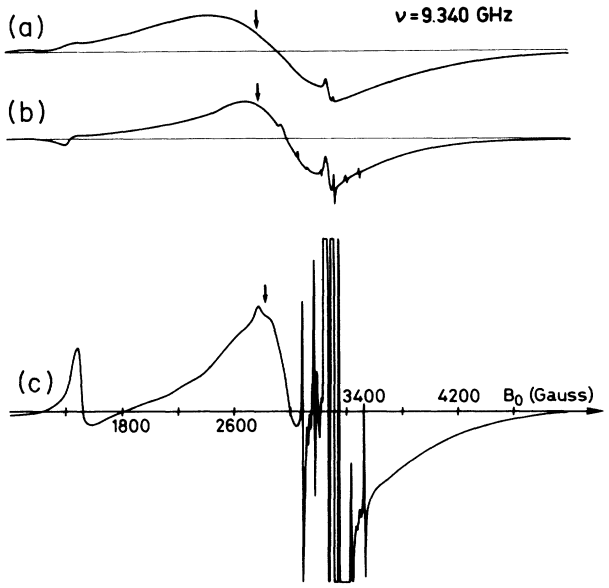

FIG. 5. ESR spectra of small MgO:Ni particles. (a) Concentration 10^{-3}, sample preparation as in Fig. 3(a). (b) Concentration 10^{-3}, sample preparation as in Fig. 3(b). (c) Concentration 10^{-4}, sample preparation as in Fig. 3(d). For a given preparation method and particle size, the Ni^{2+} linewidth varies only little with concentration between 10^{-3} and 10^{-5}. In addition to Ni^{2+} ($g=2.227$) signals are visible from Cr^{3+} ($g=1.98$, four hyperfine lines) and Mn^{2+} ($g=2.0015$, six hyperfine lines). Spectrum (c) has not been analyzed in detail. Arrows indicate the positions in the line where the data of Fig. 6 have been taken.

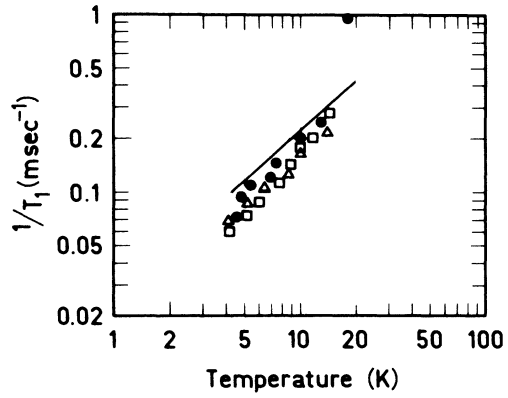

FIG. 6. Electron spin-lattice relaxation rate T_1^{-1} for Ni^{2+} in small particles of MgO. The drawn line is the theoretical prediction [see Eq. (12)] for the single crystal (cf. Fig. 2). For the purpose of the present discussion, the difference between the points and the line can be neglected. ●: Ni^{2+} concentration 10^{-4}. Sample prepared by thermal decomposition and annealed at 600°C. Average particle size 1000 Å. △: Ni^{2+} concentration 10^{-5}. Annealing at 400°C. Average particle size 270 Å. □: Ni^{2+} concentration 10^{-4}. Sample prepared by laser evaporation. Average particle size 170 Å.

data were taken. For all relaxation measurements we used a many-pulse saturation train, followed after time τ by a $\pi/2$-π readout sequence. Occasionally we verified that the result was independent of the position in the line, with the possible exception of the exact center, where double-quantum transitions can be induced. Assuming that our saturation train equalizes spin populations in all three levels ($S=1$ for Ni^{2+}), the relaxation is expected to be single exponential, as we generally find to a good approximation.

The spin-lattice relaxation in the small particles, shown in Fig. 6, is essentially equal to that in the single crystal: it does not seem warranted to discuss the slight increase in T_1 that may be indicated by the data.

IV. DISCUSSION

Not only do our samples show the presence of the direct-process spin-lattice relaxation mechanism in fine powders (from the temperature variation), but even more puzzling is the absence of any size effect on the magnitude of the dynamic spin-lattice coupling. We are unable to propose a satisfying explanation for this result, but perhaps a few remarks will help to define the nature of the problem.

The excellent agreement between theoretical and experimental spin-lattice relaxation times, taken together with the earlier cw "selective heating" experiment,[17] identify the relaxation mechanism in the bulk beyond doubt as the direct process. This indicates that 9-GHz sound waves, expected to have a wavelength of about 3200 Å, are present in equilibrium in all our samples. Although the powders in the ESR tube are certainly more dense than those on the microscope grids in Fig. 3, they have not been packed during sample preparation, and we estimate their density as an order of magnitude less than that of a single crystal.

A very important question is thus whether these samples should be considered as an ensemble of essentially independent small particles, or rather as a single structure with a considerable number of defects. In the limit of the latter case, we would use Weyl's theorem[27] to argue that the extended structure yields a $g(\omega)$ in Eq. (10) as for a crystal, and that additional modes related to the defects show up in the specific heat. In the former case, we would have to consider the important changes in dispersion relations for a small particle (the lower coordination at the surface lowers the frequencies) and the broadening of the modes due to lifetime effects. It has been found[17] that in a 3-mm crystal the acoustical phonons escape after some 5–10 encounters with the surface: if the same is true for the fundamental mode in a small crystal this says that the quality factor of this mode is only between 5 and 10, and that this broadening, together with the overall shift to lower frequencies, gives a nonzero density $g(\omega)$ in Eq. (10) (that accidentally would be equal to the bulk value).

In conclusion, there seems to be no evidence for the existence of the single-mode regime at very low frequencies

either from the present ESR experiments or from specific-heat data in the literature; size effects found so far (in calorimetric and neutron scattering experiments) (Refs. 28 and 29) belong only to the quantum size regime[1] at higher frequencies.

ACKNOWLEDGMENTS

The authors gratefully acknowledge W. Czaja, A. M. Stoneham, and W. Th. Wenckebach for many helpful discussions.

[1]H. P. Baltes and E. Simànek, in *Aerosol Microphysics II,* edited by W. H. Marlow (Springer, Berlin, 1982).

[2]C. Schaefer, Z. Phys. **7**, 287 (1921).

[3]M. Planck, *Theorie der Wärmestrahlung,* 4th ed. (Barth, Leipzig, 1921).

[4]V. Novotny and P. P. M. Meincke, Phys. Rev. B **8**, 4186 (1973).

[5]W. F. Giauque and R. C. Archibald, J. Am. Chem. Soc. **59**, 561 (1937).

[6]W. H. Lien and N. E. Phillips, J. Chem. Phys. **29**, 1415 (1958).

[7]T. H. K. Barron, W. T. Berg, and J. A. Morrison, Proc. R. Soc. London, Ser. A **250**, 70 (1959).

[8]E. Gmelin, Z. Naturforsch., Teil A **24**, 1794 (1969).

[9]E. Gmelin, Z. Naturforsch., Teil A **25**, 887 (1970).

[10]A. C. Victor, J. Chem. Phys. **36**, 2812 (1962).

[11]T. S. Chen, F. W. de Wette, L. Kleinman, and D. G. Dempsey, Phys. Rev. B **17**, 844 (1978).

[12]L. Genzel and T. P. Martin, Phys. Status Solidi B **51**, 91 (1972).

[13]H. P. Baltes and E. R. Hilf, Solid State Commun. **12**, 369 (1973).

[14]A. M. Stoneham, Solid State Commun. **3**, 71 (1965).

[15]R. Orbach and H. J. Stapleton, in *Electron Paramagnetic Resonance,* edited by S. Geschwind (Plenum, New York, 1972), p. 181.

[16]R. Orbach and H. J. Stapleton, in *Electron Paramagnetic Resonance,* edited by S. Geschwind (Plenum, New York, 1972).

[17]W. J. Brya, S. Geschwind, and G. D. Devlin, Phys. Rev. B **6**, 1924 (1972).

[18]M. F. Lewis and A. M. Stoneham, Phys. Rev. **164**, 271 (1967).

[19]B. W. Faughnan and M. W. P. Strandberg, J. Phys. Chem. Solids **19**, 155 (1961).

[20]J. W. Orton, P. Auzins, J. H. E. Griffiths, and J. E. Wertz, Proc. Phys. Soc. London **78**, 554 (1961).

[21]A. M. Stoneham, Proc. Phys. Soc. London **89**, 909 (1966).

[22]R. Gallay and J. J. van der Klink, J. Phys. E **19**, 226 (1986).

[23]J. B. Jones and M. F. Lewis, Solid State Commun. **5**, 595 (1967).

[24]J. F. Goodman, Proc. R. Soc. London, Ser. A **247**, plate 2, 346 (1958).

[25]M. Rappaz, C. Solliard, A. Châtelain, and L. A. Boatner, Phys. Rev. B **21**, 906 (1980).

[26]M. Kato, Jpn. J. Appl. Phys. **15**, 757 (1976).

[27]For a recent discussion, see H. P. Baltes and E. R. Hilf, *Spectra of Finite Systems* (Bibliographisches Institut, Mannheim, 1976).

[28]H. K. Böckelmann and R. G. Schlecht, Phys. Rev. B **10**, 5225 (1974).

[29]K. Ishikawa, N. Fujima, and H. Komura, J. Appl. Phys. **57**, 973 (1985).

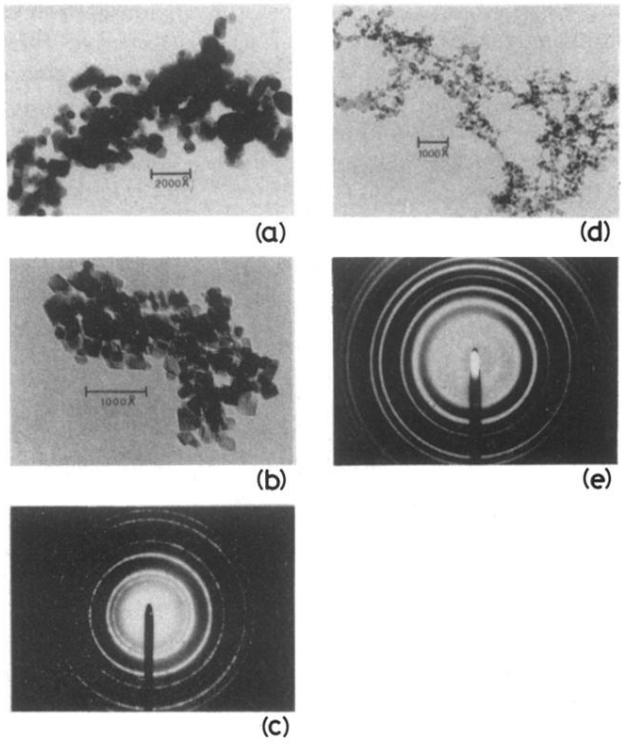

FIG. 3. Electron micrographs and diffraction rings for small-particle samples of $MgO:Ni^{2+}$ prepared by thermal decomposition and by laser evaporation. (a) Thermal decomposition and annealing at 600 °C, average particle size 1000 Å. (b) Thermal decomposition and annealing at 400 °C, average particle size 270 Å. (c) Diffraction rings of the sample shown in (a). (d) Laser evaporation, average particle size 170 Å. (e) Diffraction rings of the sample shown in (d).